

Realistic calculations of nuclear disappearance lifetimes induced by $n\bar{n}$ oscillations

E. Friedman^{1,*} and A. Gal^{1,†}

¹*Racah Institute of Physics, The Hebrew University, Jerusalem 91904, Israel*

(Dated: July 16, 2008)

Realistic calculations of nuclear disappearance lifetimes induced by $n\bar{n}$ oscillations are reported for oxygen and iron, using \bar{n} nuclear potentials derived from a recent comprehensive analysis of \bar{p} atomic X-ray and radiochemical data. A lower limit $\tau_{n\bar{n}} > 3.3 \times 10^8$ s on the $n\bar{n}$ oscillation time is derived from the Super-Kamiokande I new lower limit $T_d(O) > 1.77 \times 10^{32}$ yr on the neutron lifetime in oxygen. Antineutron scattering lengths in carbon and nickel, needed in trap experiments using ultracold neutrons, are calculated from updated \bar{N} optical potentials at threshold, with results shown to be largely model independent.

PACS numbers: 11.30.Fs, 13.75.Cs, 36.10.Gv

Keywords: neutron-antineutron oscillations, neutron lifetimes, nuclear disappearance lifetimes, antiprotonic atoms, antineutron scattering lengths

I. INTRODUCTION AND OVERVIEW

The stability of nuclei, as determined by looking for proton decay [1, 2, 3], sets a lower limit also on the lifetime of other processes such as neutron-antineutron ($n\bar{n}$) oscillations in free space. This $\Delta B = 2$ baryon-violating $n\bar{n}$ oscillation process was pointed out long ago in the pioneering papers by Kuzmin [4], by Glashow [5] and by Mohapatra and Marshak [6]. Several quantitative calculations relating the nuclear disappearance lifetime T_d to the $n\bar{n}$ oscillation time $\tau_{n\bar{n}}$ have been reported [7, 8, 9]. In these calculations a point-like $n\bar{n}$ coupling $\delta m = \hbar\tau_{n\bar{n}}^{-1}$ is assumed. In free space, δm splits the $n - \bar{n}$ degenerate mass m into mass eigenstates $m \pm \delta m$. The $n\bar{n}$ oscillations between these two mass eigenstates are suppressed in nuclear matter, giving place to decay of neutrons in a stable nucleus. Instead of two mass eigenstates one encounters two distinct widths, one which is the nuclear \bar{n} annihilation width of order $\Gamma_{\bar{n}} \approx 320$ MeV for central nuclear densities [10], the other one associated with the lifetime of a bound neutron:

$$\Gamma_d \approx \left(\frac{4 \delta m}{\Gamma_{\bar{n}}} \right) \delta m , \quad (1)$$

where $\Gamma_d = \hbar T_d^{-1}$ is the nuclear disappearance width per neutron. These statements follow, more rigorously, from a discussion of the temporal evolution of nuclear disappearance owing to $n\bar{n}$ oscillations [11]. Eq. (1) demonstrates that $n\bar{n}$ oscillations are suppressed in nuclei by 31 orders of magnitude, which is the ratio between the time scales 10^{-23} s for the strong-interaction \bar{n} annihilation time $\tau_{\bar{n}} = \hbar\Gamma_{\bar{n}}^{-1}$ and 10^8 s presumed below for the free-space oscillation time $\tau_{n\bar{n}} = \hbar(\delta m)^{-1}$. In addition to \bar{n} annihilation, neutrons and antineutrons also experience different nuclear potentials

*Electronic address: elifried@vms.huji.ac.il

†Electronic address: avragal@vms.huji.ac.il

U_n and $U_{\bar{n}}$, leading within a closure approximation [12] to a refinement of Eq. (1):

$$\Gamma_d^{\text{closure}} \approx \Gamma_{\bar{n}} \frac{(\delta m)^2}{<W_{\bar{n}}>^2 + <(U_{\bar{n}} - U_n)>^2}, \quad (2)$$

where $<W_{\bar{n}}> = \Gamma_{\bar{n}}/2$ is some appropriately chosen average of (minus) the imaginary part of the \bar{n} nuclear potential.

To leading order, from Eq. (1), the relationship between $\tau_{n\bar{n}}$ and T_d is given roughly by

$$\tau_{n\bar{n}} \approx 2 (\hbar T_d / \Gamma_{\bar{n}})^{1/2}. \quad (3)$$

The values reported for T_d in the literature, by convention, are normalized per neutron and take into account secondary and absorption processes. Thus, T_d essentially stands for the lifetime of a neutron in a stable nucleus. Using the best value $T_d(\text{Fe}) > 7.2 \times 10^{31}$ yr published by the Soudan 2 Collaboration [3], Eq. (3) gives a lower limit estimate of $\tau_{n\bar{n}} > 1.4 \times 10^8$ s. This estimate is to be compared with the lower limit $\tau_{n\bar{n}} > 1.3 \times 10^8$ s stated by the Soudan 2 Collaboration using the calculations made long ago by Dover-Gal-Richard [8]. However, this apparent agreement might be fortuitous. We comment that the lower limit on $\tau_{n\bar{n}}$ derived from nuclear disappearance considerations is higher than that determined using nuclear-reactor neutrons directly in searches for $n\bar{n}$ oscillations. The lower limit given by the Grenoble reactor experiment [13] is $\tau_{n\bar{n}} > 0.86 \times 10^8$ s.

Recently, the Super-Kamiokande (SK) collaboration released an improved value for T_d in oxygen, $T_d(\text{O}) > 1.77 \times 10^{32}$ yr [14]. In the present work we report an accurate calculation of the lower limit on $\tau_{n\bar{n}}$ implied by this value of $T_d(\text{O})$, using the latest detailed analysis by our group which derived antinucleon nuclear potentials from antiprotonic atom data and radiochemical data [10]. These potentials are essentially isoscalar and apply to antineutrons as well as to antiprotons. For completeness, in this study we also calculate the reduced lifetime (see below) in iron which will provide the necessary link between a future measurement of $T_d(\text{Fe})$ and a derivation of a lower limit on $\tau_{n\bar{n}}$.

Another experimental method of looking for $n\bar{n}$ oscillations is to use ultracold neutrons in a trap, first suggested by Chetyrkin *et al.* [12] and discussed since then by several other groups, *e.g.* in Refs. [15, 16]. A necessary input for interpreting such experiments are the nuclear \bar{n} scattering lengths for ultracold antineutrons in matter. We report here on calculations of \bar{n} scattering lengths for several chosen materials, again based on the analysis of antiprotonic atoms. The calculated values of these scattering lengths turn out to be largely model independent owing to the strong absorption of low energy antinucleons.

II. METHODOLOGY

A. Wave equations, widths and lifetime

A point-like coupling $\delta m = \hbar\tau_{n\bar{n}}^{-1}$, representing $n\bar{n}$ oscillations in free space, connects each of the stationary bound single-particle (sp) neutron states to the corresponding \bar{n} stationary sp state. The sp energies assume complex values $E_{\nu\ell j} = -B_{\nu\ell j} - i\Gamma_{\nu\ell j}/2$, where the imaginary part of the energy in the sp state labeled $\nu\ell j$ gives the disappearance width $\Gamma_{\nu\ell j}$ for this state. The coupled $n\bar{n}$ radial wave equations for the neutron sp wavefunction $u_{\nu\ell j}(r)$ and the antineutron sp wavefunction $w_{\nu\ell j}(r)$ are given by

$$-\frac{\hbar^2}{2\mu} u_{\nu\ell j}''(r) + \frac{\hbar^2\ell(\ell+1)}{2\mu r^2} u_{\nu\ell j}(r) - U_n(r) u_{\nu\ell j}(r) - E_{\nu\ell j} u_{\nu\ell j}(r) + \delta m w_{\nu\ell j}(r) = 0, \quad (4)$$

$$-\frac{\hbar^2}{2\mu} w_{\nu\ell j}''(r) + \frac{\hbar^2\ell(\ell+1)}{2\mu r^2} w_{\nu\ell j}(r) - [U_{\bar{n}}(r) + i W_{\bar{n}}(r)] w_{\nu\ell j}(r) - E_{\nu\ell j} w_{\nu\ell j}(r) + \delta m u_{\nu\ell j}(r) = 0 , \quad (5)$$

where $-U_n(r)$ and $-(U_{\bar{n}}(r) + i W_{\bar{n}}(r))$ are the nuclear potentials exerted by the nuclear core on the neutrons and antineutrons, respectively, and μ is the reduced mass. The radial wavefunctions $u_{\nu\ell j}(r)$ and $w_{\nu\ell j}(r)$ are regular at the origin and decay with r outside of the nucleus. A useful expression for the width $\Gamma_{\nu\ell j}$ is obtained by multiplying Eq. (4) by $u_{\nu\ell j}^*(r)$, and the complex conjugate of Eq. (4) by $u_{\nu\ell j}(r)$, subtracting the resulting expressions from each other and integrating from zero to infinity. The result is

$$\Gamma_{\nu\ell j} = -\frac{2 \delta m \int \text{Im} (w_{\nu\ell j}(r) u_{\nu\ell j}^*(r)) dr}{\int |u_{\nu\ell j}(r)|^2 dr} . \quad (6)$$

The initial-time boundary condition of no antineutrons implies that $|w/u| = O(\delta m/B)$, where the binding energy B represents any of the strong-interaction entities, such as $\Gamma_{\bar{n}}$ [11]. It follows then from Eq. (6) that the width Γ is of order $(\delta m)^2/\Gamma_{\bar{n}}$, in agreement with Eq. (1). The terms with Γ and δm in Eq. (4) are negligible, of order $(\delta m/B)^2$ with respect to the rest of the terms which coincide with those constituting a stable bound-neutron radial wave equation in which $B_{\nu\ell j} = B_{\nu\ell j}^{(n)}$ stands for the neutron sp binding energy. Thus, the solutions $u_{\nu\ell j}$ are essentially real functions. Eq. (6) expresses a relationship between these two minute terms which are neglected below. Turning to Eq. (5), all terms there are of the same order, except for the Γ term which is of order $(\delta m/B)^2$ with respect to the other terms and, hence, may be dropped off.

Dropping off the terms of order $(\delta m/B)^2$ in Eqs. (4) and (5), we obtain the radial equations satisfied (i) by a bound-neutron wavefunction,

$$-\frac{\hbar^2}{2\mu} u_{\nu\ell j}''(r) + \frac{\hbar^2\ell(\ell+1)}{2\mu r^2} u_{\nu\ell j}(r) - U_n(r) u_{\nu\ell j}(r) + B_{\nu\ell j}^{(n)} u_{\nu\ell j}(r) = 0 , \quad (7)$$

and (ii) by a quasibound antineutron *reduced* wavefunction $v_{\nu\ell j}(r) = w_{\nu\ell j}(r)/\delta m$,

$$-\frac{\hbar^2}{2\mu} v_{\nu\ell j}''(r) + \frac{\hbar^2\ell(\ell+1)}{2\mu r^2} v_{\nu\ell j}(r) - [U_{\bar{n}}(r) + i W_{\bar{n}}(r)] v_{\nu\ell j}(r) + B_{\nu\ell j}^{(n)} v_{\nu\ell j}(r) + u_{\nu\ell j}(r) = 0 . \quad (8)$$

Operating on Eq. (8) similarly to the way in which Eq. (6) was derived from Eq. (4), recalling that $B_{\nu\ell j}^{(n)}$ and $u_{\nu\ell j}(r)$ are real, and multiplying the result by $(\delta m)^2$ in order to make connection with Eq. (6), we obtain

$$-2(\delta m)^2 \int \text{Im} (v_{\nu\ell j}(r) u_{\nu\ell j}^*(r)) dr = 2(\delta m)^2 \int W_{\bar{n}}(r) |v_{\nu\ell j}(r)|^2 dr , \quad (9)$$

so that the disappearance width from the $\nu\ell j$ sp state, Eq. (6), is given by

$$\Gamma_{\nu\ell j} = \frac{2(\delta m)^2 \int W_{\bar{n}}(r) |v_{\nu\ell j}(r)|^2 dr}{\int u_{\nu\ell j}^2(r) dr} = -\frac{2(\delta m)^2 \int u_{\nu\ell j}(r) \text{Im} v_{\nu\ell j}(r) dr}{\int u_{\nu\ell j}^2(r) dr} \quad (10)$$

in terms of the solutions $u_{\nu\ell j}$ and $v_{\nu\ell j}$ of Eqs. (7) and (8), respectively. The averaged disappearance width *per neutron* is then given by

$$\Gamma_d = \frac{1}{N} \sum n_{\nu\ell j} \Gamma_{\nu\ell j} , \quad (11)$$

where $n_{\nu\ell j}$ is the appropriate number of neutrons in the sp state $\nu\ell j$, $N = \sum n_{\nu\ell j}$ is the number of neutrons in the decaying nucleus and summation is over the occupied neutron sp states. Since Γ_d scales as $(\delta m)^2$, hence inversely proportional to $\tau_{n\bar{n}}^2$, it is customary to define a *reduced lifetime* T_R given by

$$T_R = \frac{\hbar}{\Gamma_d \tau_{n\bar{n}}^2} , \quad (12)$$

which has dimension of inverse time (s^{-1}). The nuclear disappearance lifetime T_d is then given by

$$T_d = \frac{\hbar}{\Gamma_d} = T_R \tau_{n\bar{n}}^2. \quad (13)$$

We solve numerically both Eqs. (7) and (8) for neutron and antineutron sp states, respectively. Eq. (7) is identical with that used in nuclear bound state problems for occupied sp neutron states. Eq. (8) is solved for each one of the antineutron sp states with reduced wavefunctions $v_{\nu\ell j}$ that are generated by the corresponding occupied sp neutron wavefunctions $u_{\nu\ell j}$ acting as an inhomogeneous source. The solutions $u_{\nu\ell j}$ and $v_{\nu\ell j}$ serve as input in the integrals Eq. (10) for the widths $\Gamma_{\nu\ell j}$. For completeness we note the precise expression for $\Gamma_{\nu\ell j}$, without neglecting contributions of order $(\delta m/B)^2$:

$$\Gamma_{\nu\ell j} = \frac{2 \int W_{\bar{n}}(r) |w_{\nu\ell j}(r)|^2 dr}{\int (|u_{\nu\ell j}(r)|^2 + |w_{\nu\ell j}(r)|^2) dr}, \quad (14)$$

where $u_{\nu\ell j}$ and $w_{\nu\ell j}$ solve Eqs. (4) and (5).

B. Nuclear structure issues

The standard shell-model (SM) description of neutron sp states in nuclei introduces spurious excitations of the center of mass degree of freedom. It is important, particularly in as light a nucleus as ^{16}O , to eliminate this spuriousity and thus avoid its unphysical effects on the equations solved for the neutron sp states and on the neutron disappearance widths subsequently derived. A general construction of translationally invariant (TI) nuclear wavefunctions and densities, in the harmonic-oscillator basis, was given by Navrátil [17]. Here we follow the earlier discussion by Millener *et al.* [18] which is specifically suited to the p shell. Solving radial equations in the relative coordinate between a neutron and its nuclear core in a p -shell nucleus, the number of neutrons in the s shell and p shell has to be modified from the SM values $n_{1s}^{\text{SM}} = 2$ and $n_{1p}^{\text{SM}} = (N - 2)$ to

$$n_{1s}^{\text{TI}} = 2 - \frac{N - 2}{A - 1}, \quad n_{1p}^{\text{TI}} = \frac{A}{A - 1}(N - 2), \quad (15)$$

where for $N = 8$ appropriate to ^{16}O we have $n_{1s}^{\text{TI}} = 1.6$ and $n_{1p}^{\text{TI}} = 6.4$. To reproduce a given value of the mean-square (ms) radius of the point-neutron distribution $\langle r^2 \rangle_n$, the ms radii of the neutron-core $1s$ and $1p$ wavefunctions have to satisfy

$$\langle r^2 \rangle_n = \frac{1}{N} \left(\frac{A - 1}{A} \right)^2 (n_{1s}^{\text{TI}} \langle r^2 \rangle_{1s} + n_{1p}^{\text{TI}} \langle r^2 \rangle_{1p}), \quad (16)$$

where it was assumed that the s -hole and p -hole strengths are not fragmented. In practice we used a spin-orbit potential to split the p -hole strength according to the observed $p_{1/2} - p_{3/2}$ energy difference. Equation (16) is to be contrasted with the SM version in which center of mass spuriousities are disregarded:

$$\langle r^2 \rangle_n = \frac{1}{N} (n_{1s}^{\text{SM}} \langle r^2 \rangle_{1s} + n_{1p}^{\text{SM}} \langle r^2 \rangle_{1p}). \quad (17)$$

C. Numerical solution

The real wavefunction $u_{\nu\ell j}$ for the bound neutron is obtained by solving numerically Eq. (7) using a standard method. Here we describe briefly the method used to solve the inhomogenous equation (8) for the quasibound antineutron reduced wavefunction in the potential taken from fits to antiprotonic atom data [10].

The inhomogeneous radial equation (8) is integrated numerically from $r = 0$ outward using the Numerov method, requiring the usual regular boundary condition $v_{\nu\ell j} \sim r^{\ell+1}$ at the origin. In parallel, the corresponding homogeneous radial equation

$$-\frac{\hbar^2}{2\mu} v_{\nu\ell j}^{(0)''}(r) + \frac{\hbar^2 \ell(\ell+1)}{2\mu r^2} v_{\nu\ell j}^{(0)}(r) - [U_{\bar{n}}(r) + i W_{\bar{n}}(r)] v_{\nu\ell j}^{(0)}(r) + B_{\nu\ell j}^{(n)} v_{\nu\ell j}^{(0)}(r) = 0 , \quad (18)$$

obtained from Eq. (8) by omitting the last term, is also integrated using the regular boundary condition at $r = 0$. Integration is carried out to a matching radius R where the nuclear \bar{n} potentials may safely be neglected. Both integrations lead to exponentially increasing functions toward R , as expected. The most general, regular at $r = 0$ solution of Eq. (8) is given by the linear combination

$$v_{\nu\ell j}^< = a_{\nu\ell j} v_{\nu\ell j}^{(0)} + v_{\nu\ell j} , \quad (19)$$

where the (complex) constant $a_{\nu\ell j}$ is chosen such that $v_{\nu\ell j}^<$ is regular also at infinity.

We note that outside the matching radius R the homogeneous equation (18) is satisfied by the neutron bound-state wavefunction $u_{\nu\ell j}$. The most general, regular at $r \rightarrow \infty$ solution of Eq. (8) is then given by the linear combination

$$v_{\nu\ell j}^> = b_{\nu\ell j} u_{\nu\ell j} + \tilde{v}_{\nu\ell j} , \quad (20)$$

where $\tilde{v}_{\nu\ell j}$ is a special, regular at $r \rightarrow \infty$ solution of the inhomogeneous equation (8), and $b_{\nu\ell j}$ is an arbitrary (complex) constant.

The constants $a_{\nu\ell j}$ and $b_{\nu\ell j}$ above are determined by requiring that the ‘inside’ and ‘outside’ solutions, $v_{\nu\ell j}^<$ and $v_{\nu\ell j}^>$ respectively, as well as their first derivatives, agree with each other at the matching point $r = R$. We note that for the purpose of evaluating the disappearance widths $\Gamma_{\nu\ell j}$, only the knowledge of the constants $a_{\nu\ell j}$ is required. A straightforward algebra gives

$$a_{\nu\ell j} = \frac{[u'_{\nu\ell j}(R)\tilde{v}_{\nu\ell j}(R) - u_{\nu\ell j}(R)\tilde{v}'_{\nu\ell j}(R)] - [u'_{\nu\ell j}(R)v_{\nu\ell j}(R) - u_{\nu\ell j}(R)v'_{\nu\ell j}(R)]}{u'_{\nu\ell j}(R)v_{\nu\ell j}^{(0)}(R) - u_{\nu\ell j}(R)v_{\nu\ell j}^{(0)'}(R)} . \quad (21)$$

Since both $u_{\nu\ell j}$ and $\tilde{v}_{\nu\ell j}$ fall off exponentially, whereas $v_{\nu\ell j}$ increases exponentially at R , the terms in the first square bracket in the numerator of Eq. (21) are of order $\exp(-2\kappa_{\nu\ell j}R)$ with respect to the terms in the second square bracket, and may be safely neglected. Here $\kappa_{\nu\ell j} = (2\mu B_{\nu\ell j}^{(n)})^{1/2}/\hbar$, and $\exp(-2\kappa_{\nu\ell j}R) < 10^{-4}$ for a wide range of realistic nuclear applications. Hence, to such high accuracy

$$a_{\nu\ell j} \approx -\frac{u'_{\nu\ell j}(R)v_{\nu\ell j}(R) - u_{\nu\ell j}(R)v'_{\nu\ell j}(R)}{u'_{\nu\ell j}(R)v_{\nu\ell j}^{(0)}(R) - u_{\nu\ell j}(R)v_{\nu\ell j}^{(0)'}(R)} , \quad (22)$$

and no specific knowledge of the special solutions $\tilde{v}_{\nu\ell j}$ is required. [Special solutions $\tilde{v}_{\nu\ell j}$ in terms of neutron wavefunctions $u_{\nu\ell j}$ are given in the Appendix.] A further simplification of Eq. (22) occurs by noting that $v_{\nu\ell j}$ in the numerator and $v_{\nu\ell j}^{(0)}$ in the denominator, for any given ℓ value, share the same asymptotic behavior at R , which leads to the final result

$$a_{\nu\ell j} \approx -\frac{v_{\nu\ell j}(R)}{v_{\nu\ell j}^{(0)}(R)} . \quad (23)$$

These expressions are useful only when their dependence on the matching radius R is negligible. In practice we used Eq. (22) with radial integration steps of 0.04 fm and R between 10 and 13 fm. The coefficients $a_{\nu\ell j}$ which determine

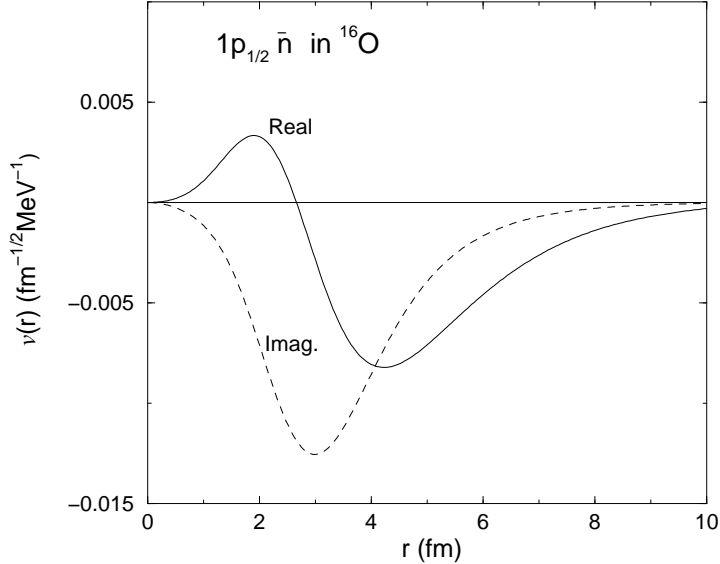


FIG. 1: Antineutron $1p_{1/2}$ reduced radial wavefunction v in ^{16}O .

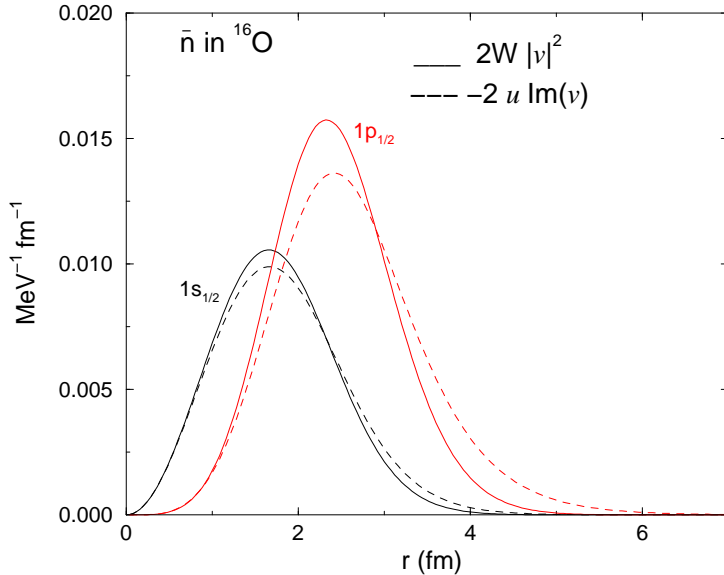


FIG. 2: Integrands in the numerators for the two versions of the neutron disappearance width Eq. (10).

the required decaying \bar{n} radial wavefunctions in the region $r < R$ were found to vary by less than 10^{-5} of their values, with the resulting widths stable to better than 10^{-4} . Both forms of Eq. (10) gave identical results to this order. The same accuracy is also obtained using Eq. (23). For comparison with previous calculations, we calculated the widths for ^{16}O , using the input parameters given by Dover *et al.* [8]. The results agreed with those listed in Table I of that reference to within 1%.

Figure 1 shows, as an example, the reduced antineutron $1p_{1/2}$ wavefunction v in ^{16}O . Note that the longer tail of the real part is of no consequence for the disappearance width because in the $|v_{\nu\ell j}(r)|^2$ version of the integral, Eq. (10), the imaginary potential W is of a shorter range. The other version of the width contains only the imaginary part

TABLE I: Calculated reduced neutron disappearance widths $\Gamma_{\nu\ell j}/(\delta m)^2$ (in MeV $^{-1}$).

state $\nu\ell j$	$n_{\nu\ell j}^{\text{SM}}$	$n_{\nu\ell j}^{\text{TI}}(^{16}\text{O})$	$^{16}\text{O}(\text{SM})$	$^{16}\text{O}(\text{TI})$	$^{56}\text{Fe}(\text{SM})$
$1s_{1/2}$	2	1.6000	0.0207	0.0220	0.0144
$1p_{3/2}$	4	4.2667	0.0296	0.0296	0.0177
$1p_{1/2}$	2	2.1333	0.0321	0.0343	0.0177
$1d_{5/2}$	6	—	—	—	0.0217
$2s_{1/2}$	2	—	—	—	0.0238
$1d_{3/2}$	4	—	—	—	0.0219
$1f_{7/2}$	8	—	—	—	0.0268
$2p_{3/2}$	2	—	—	—	0.0343
$\Gamma_d/(\delta m)^2$ -average [Eq. (11)]			0.0280	0.0294	0.0228
$\Gamma_d/(\delta m)^2$ -closure [Eq. (2)]			0.0271	0.0265	0.0220
T_R [Eq. (12) (s $^{-1}$)			0.543×10^{23}	0.517×10^{23}	0.666×10^{23}

of the antineutron wavefunction, which is of a shorter range as is seen in the figure. Figure 2 shows the integrands in the numerator for the two versions of the width, for $1s_{1/2}$ and $1p_{1/2}$ neutrons in ^{16}O . It is remarkable that the relative differences between the integrals are less than 10^{-5} , although the two integrands are not identical both near the maxima and in the tail region.

III. RESULTS

A. Neutron disappearance widths

Neutron disappearance widths for the various subshells $\nu\ell j$ were calculated for ^{16}O and ^{56}Fe with the two forms given by Eq. (10). The bound neutron wavefunctions $u_{\nu\ell j}$ were calculated in a Woods-Saxon potential $-U_0^{(n)}/[1 + \exp((r - R_{1/2})/a)]$ whose depth $U_0^{(n)}$ was adjusted in each nucleus to fit the experimental separation energy of the least-bound neutron. A spin-orbit term was added to reproduce the observed $p_{1/2} - p_{3/2}$ splitting. The half-density radius parameters $R_{1/2} = r_0(A - 1)^{1/3}$ were adjusted such that the root-mean-square (rms) radius of the whole neutron distributions was 2.57 fm for ^{16}O and 3.71 fm for ^{56}Fe . For ^{16}O it corresponds to the known rms radius for the point-proton distribution and for ^{56}Fe it is 0.09 fm larger than the known value for the point-proton distribution [19]. The diffusivity parameter a was fixed at $a = 0.60$ fm for ^{16}O and $a = 0.55$ fm for ^{56}Fe . Using Eq. (17) for ^{16}O and its straightforward extension for ^{56}Fe , values of $r_0 = 1.325$ fm and $r_0 = 1.304$ fm were found for the SM calculations in ^{16}O and ^{56}Fe , respectively, whereas using Eq. (16) a value of $r_0 = 1.442$ fm was found for the TI calculation in ^{16}O . The depths of the SM potential were 53.8 MeV for ^{16}O and 51.1 MeV for ^{56}Fe , and the depth of the TI potential in ^{16}O was 48.8 MeV. For the antineutrons we used the most recent phenomenological isoscalar potential obtained from large-scale ('global') fits to 90 data points of strong-interaction shifts and widths in antiprotonic atoms across the periodic table [10]. The effective amplitude for that potential is $b_0 = 1.3 + i 1.9$ fm, used with a finite-range Gaussian folded with a range parameter 0.9 fm into the nuclear matter density; see Ref. [10] for more details. These potentials are shown in Fig. 3 and Fig. 4 for $\bar{n}-^{15}\text{O}$ and $\bar{n}-^{55}\text{Fe}$, respectively.

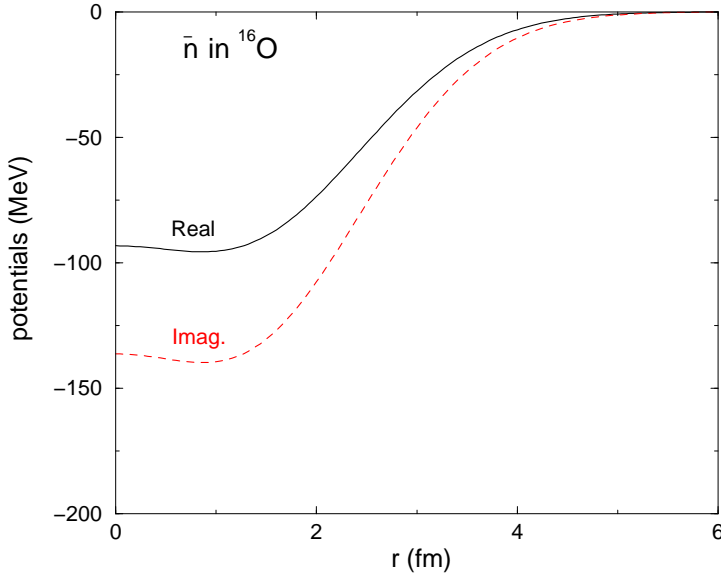


FIG. 3: The antineutron optical potential in ^{16}O .

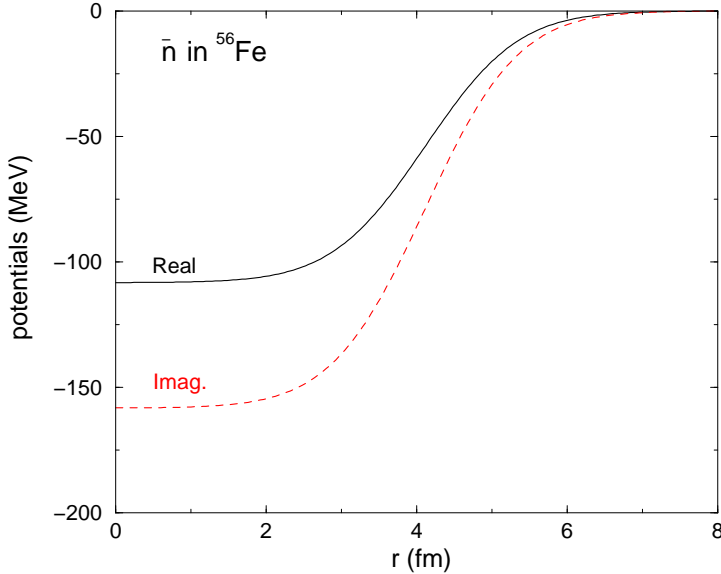


FIG. 4: The antineutron optical potential in ^{56}Fe .

The neutron disappearance widths as given by Eq. (10) scale with $(\delta m)^2$. Therefore in Table I we list the calculated reduced neutron disappearance widths $\Gamma_{\nu\ell j}/(\delta m)^2$ for the various sub-shells in ^{16}O and in ^{56}Fe . These calculated widths increase by as much as 50% in ^{16}O and by over 100% in ^{56}Fe going outward from the inner $1s_{1/2}$ sp neutron state to the least-bound sp neutron state, in agreement with the trend found in earlier calculations [8]. The values of $\Gamma_d/(\delta m)^2$ calculated using the closure expression Eq. (2) give excellent approximation to the exact weighted averages, provided values of the nuclear potentials U_n , $U_{\bar{n}}$, $W_{\bar{n}}$ at the nuclear surface, here approximated by half of the corresponding values at the center of the nucleus, are adopted. We comment that for the strongly absorptive \bar{n} potential used by us, the effect of the real potentials U_n and $U_{\bar{n}}$ is secondary to that of the imaginary potential $W_{\bar{n}}$.

TABLE II: \bar{n} scattering lengths a (in fm) from fits to \bar{p} atomic data.

Nucleus	FR [10]	ZR [10]	Eq. (24)	S [22]	D [22]
^{12}C	$3.26 - i 0.97$	$3.21 - i 0.84$	$(3.34 \pm 0.07) - i (1.00 \pm 0.04)$	$3.16 - i 0.87$	$3.11 - i 1.10$
^{58}Ni	$5.41 - i 1.12$	$5.43 - i 1.14$	$(5.44 \pm 0.11) - i (1.00 \pm 0.04)$		

A more elaborate averaging with the nuclear density should give similar results for strongly absorptive \bar{n} potentials, as found by Dover *et al.* [8]. As for using the TI or the SM schemes for ^{16}O , the difference between the averaged widths, or between the reduced lifetimes, amounts to merely 5% which affects the limit placed on $\tau_{n\bar{n}}$ to only 2.5%. Our calculated values of the reduced lifetimes T_R are smaller than those calculated in Ref. [8]. This difference reflects partly the difference in the \bar{n} potentials used and partly the more precise treatment of the nuclear geometry in our calculations. The half-density radius parameter of the WS potential used by Dover *et al.* in the SM calculation for ^{16}O was taken as $R_{1/2} = 2.545$ fm, whereas it assumes the value $R_{1/2} = 3.268$ fm in the present SM calculation for ^{16}O . The values of $R_{1/2}$ used for ^{56}Fe are very close to each other in these works. Finally, for the recently reported SK result, $T_d(\text{O}) > 1.77 \times 10^{32}$ yr [14] in oxygen, our calculated value for the reduced neutron disappearance width, using the TI version, implies a lower limit of $\tau_{n\bar{n}} > 3.3 \times 10^8$ s.

B. Antineutron scattering lengths

For ultracold neutron experiments searching for $n\bar{n}$ oscillations, the knowledge of their scattering lengths in a given material is essential for constructing the relevant Fermi pseudopotentials. The neutron scattering lengths are known from thermal neutron reactions. Here we discuss the extraction of antineutron scattering lengths from the \bar{p} optical potentials determined from a comprehensive analysis of \bar{p} atomic data. We note that for the best-fit \bar{p} potentials, the isovector component came out negligible [10], so the \bar{n} and \bar{p} potentials are identical. Antinucleon scattering lengths were discussed extensively in Ref. [20]. It was found there that a simple global parameterization was possible, in the form

$$\text{Re } a = (1.54 \pm 0.03) A^{0.311 \pm 0.005} \text{ fm} , \quad \text{Im } a = -1.00 \pm 0.04 \text{ fm} , \quad (24)$$

for $A > 10$. The approximate $A^{1/3}$ dependence of the real part, and the constancy of imaginary part, are to be expected on the basis of a simple model based on a strongly absorptive square well potential, although the actual magnitude of $\text{Im } a$ is considerably larger than expected for a sharp-edge potential, resulting mainly from the diffuseness of the potential [21].

In our latest work [10] the data base has been extended to include the numerous CERN PS209 Collaboration \bar{p} atomic data. The values of a due to the isoscalar \bar{N} potentials fitted to this extended set of data are listed for ^{12}C and ^{58}Ni in Table II, together with values obtained using Eq. (24), and also from the earlier work by Wong *et al.* [22]. Here, FR and ZR stand for values of a derived from best global-fit finite-range and zero-range potentials, respectively, with FR giving the lowest χ^2 [10]. The notations S (shallow) and D (deep) stand for values of a calculated in Ref. [15] from potentials with a relatively weak absorptivity W or a strong one, respectively, derived from limited fits in Ref. [22]. The resulting scattering lengths a exhibit a remarkable independence of the model used, provided it fits the \bar{p} atomic

data. This stability follows from the strong absorptivity of the \bar{p} potential which suppresses the associated $1s$ atomic radial wavefunction in the nuclear interior where the main model dependence arises [23].

IV. SUMMARY

We have reported results of precise calculations of the reduced lifetimes of representative nuclei, ^{16}O and ^{56}Fe , against neutron-antineutron oscillations, thus providing revised and updated lower limits on the free-space $n\bar{n}$ oscillation time $\tau_{n\bar{n}}$. The best lower limit is now provided by the very recent SK measurement [14] in ^{16}O which yields according to our calculation a limit of $\tau_{n\bar{n}} > 3.3 \times 10^8$ s. We have used the latest (isoscalar) antinucleon potentials derived from the analysis of a large-scale set of \bar{p} atomic data near threshold [10]. Having solved accurately the sp equations for neutrons and (coupled) antineutrons, it became possible to test the usefulness of rough approximations such as Eq. (2) in terms of mean nuclear potentials for neutrons and antineutrons. We found that using surface values for these mean potentials, taken as half the corresponding values in the center of the nucleus, provided an excellent approximation to the exact calculation. This points out to a considerably mild model dependence of the calculated reduced widths that are sensitive foremost to \bar{n} potentials at the nuclear surface where their determination from \bar{p} atomic data involves only little extrapolation.

An educated estimate of the *theoretical* uncertainty involved in the derivation of the lower bound deduced in the present work on the $n\bar{n}$ oscillation time $\tau_{n\bar{n}}$ can be made as follows.

- For a given nucleus like ^{16}O and a given \bar{n} -nuclear potential, but considering alternative ways of treating the nuclear size, the calculated nuclear widths vary by 5% (columns 4 and 5 of Table I), so the uncertainty in the derived $\tau_{n\bar{n}}$ is about 2.5%.
- The uncertainty arising from using different nuclei (columns 4 and 6 of Table I) comes mostly from the uncertainty in the strength of the absorptive (imaginary) \bar{n} -nuclear potential. That shows about 20% uncertainty for the averaged disappearance width Γ_d , and hence 10% for $\tau_{n\bar{n}}$.

Thus, the overall theoretical uncertainty involved in the present *one-nucleon* $n\bar{n}$ oscillation calculations is about 10% – 15%. It should be viewed as a model-dependence uncertainty that is considerably lower than the 50% – 100% uncertainty range evident in many of the calculations from the 1980s and 1990s, *e.g.* Ref. [8], before the information from \bar{p} atoms became as abundant and precise as it is available to date [10]. Other past calculations [7, 9] which avoided using \bar{n} phenomenological optical potentials faced a tougher task of having to renormalize the $\bar{n}N$ strong interaction within the nucleus, a formidable job that was bypassed by Dover *et al.* [8] and in the present work using a well-constrained phenomenological \bar{n} -nuclear potential.

Another source of uncertainty involves *two-nucleon* processes which inside the nucleus might compete with the leading one-nucleon process considered here. In their 1985 paper, making contact with beta-decay and EMC calculations, Dover *et al.* [8] estimated these additional modes of neutron disappearance to be about 15% – 30%, and largely incoherent with the one-nucleon mode. This provides a *systematical* uncertainty which may be used to *increase* the stated lower bound on $\tau_{n\bar{n}}$.

Acknowledgments

One of us (A.G.) thanks Yuri Kamshkov for his support and hospitality during the International Workshop on B-L Violation, Berkeley, September 2007, where a related preliminary presentation was made. We thank John Millener for useful correspondence on translationally invariant nuclear wavefunctions. This research was partially supported by the Israel Science Foundation grant 757/05.

Appendix: asymptotic \bar{n} radial wavefunctions

Here we record special, regular at $r \rightarrow \infty$ solutions of the \bar{n} inhomogeneous radial Eq. (8) in terms of similar solutions of the n homogeneous radial Eq. (7). At $r > R$, where the \bar{n} and n nuclear potentials are negligible, these equations are written in standard form as

$$-v_{\nu\ell j}''(\rho) + \frac{\ell(\ell+1)}{\rho^2}v_{\nu\ell j}(\rho) + v_{\nu\ell j}(\rho) + \frac{1}{B_{\nu\ell j}^{(n)}}u_{\nu\ell j}(\rho) = 0 , \quad (25)$$

$$-u_{\nu\ell j}''(\rho) + \frac{\ell(\ell+1)}{\rho^2}u_{\nu\ell j}(\rho) + u_{\nu\ell j}(\rho) = 0 , \quad (26)$$

for \bar{n} and n , respectively, where $\rho = \kappa_{\nu\ell j}r$ is dimensionless. The n bound-state, regular at $\rho \rightarrow \infty$ solutions are given by

$$u_{\nu\ell j}(\rho) = A_{\nu\ell j}\mathcal{P}_\ell(\rho)\exp(-\rho) = A_{\nu\ell j}(-1)^\ell \rho^{\ell+1} \left(\frac{1}{\rho} \frac{d}{d\rho}\right)^\ell \frac{\exp(-\rho)}{\rho} , \quad (27)$$

where $A_{\nu\ell j}$ are normalization constants ensuring that asymptotically $\mathcal{P}_\ell(\rho \rightarrow \infty) \rightarrow 1$. $\mathcal{P}_\ell(\rho)$ are polynomials in $1/\rho$, related to the outgoing spherical Hankel functions [24], satisfying the differential equation

$$\mathcal{P}_\ell''(\rho) - 2\mathcal{P}_\ell'(\rho) - \frac{\ell(\ell+1)}{\rho^2}\mathcal{P}_\ell(\rho) = 0 . \quad (28)$$

The lowest-order \mathcal{P}_ℓ s relevant to the present work are

$$\mathcal{P}_0(\rho) = 1 , \quad \mathcal{P}_1(\rho) = (1 + \frac{1}{\rho}) , \quad \mathcal{P}_2(\rho) = (1 + \frac{3}{\rho} + \frac{3}{\rho^2}) , \quad \mathcal{P}_3(\rho) = (1 + \frac{6}{\rho} + \frac{15}{\rho^2} + \frac{15}{\rho^3}) . \quad (29)$$

A useful recursion relation satisfied by the \mathcal{P}_ℓ s is

$$\mathcal{P}_\ell(\rho) = (1 + \frac{\ell}{\rho})\mathcal{P}_{\ell-1}(\rho) - \mathcal{P}_{\ell-1}'(\rho) \quad (\mathcal{P}_{-1}(\rho) \equiv 1) , \quad (30)$$

easily derived from the explicit form of \mathcal{P}_ℓ given in Eq. (27).

It can be shown that regular at $\rho \rightarrow \infty$ solutions of the \bar{n} inhomogeneous radial Eq. (25) are given by

$$v_{\nu\ell j}(\rho) = -\frac{A_{\nu\ell j}}{2B_{\nu\ell j}^{(n)}} \rho \mathcal{Q}_\ell(\rho)\exp(-\rho) , \quad (31)$$

where $\mathcal{Q}_\ell(\rho) = \mathcal{P}_{\ell-1}(\rho)$. For a proof, one forms the inhomogeneous second-order differential equation satisfied by the \mathcal{Q}_ℓ s, making use of Eqs. (28) and (30). The latter equation allows us then to construct the \mathcal{Q}_ℓ s recursively:

$$\mathcal{Q}_{\ell+1}(\rho) = (1 + \frac{\ell}{\rho})\mathcal{Q}_\ell(\rho) - \mathcal{Q}_\ell'(\rho) \quad (\mathcal{Q}_0(\rho) = 1) . \quad (32)$$

[1] M. Takita *et al.* (Kamiokande Collaboration), Phys. Rev. D **34**, 902 (1986).

[2] Ch. Berger *et al.* (Frèjus Collaboration), Phys. Lett. B **240**, 237 (1990).

[3] J. Chung *et al.* (Soudan 2 Collaboration), Phys. Rev. D **66**, 032004 (2002).

[4] V.A. Kuzmin, JETP Lett. **12**, 335 (1970) [English translation: *ibid.* **12**, 228 (1970)].

[5] S.L. Glashow, in *Neutrino '79, Proc. Int. Conf. Neutrinos, Weak Interactions and Cosmology, Bergen, Norway, 1979*, Eds. A. Haatuft and C. Jarlskog (Univ. Bergen, Bergen, 1980), Vol. 2, p. 518.

[6] R.N. Mohapatra and R.E. Marshak, Phys. Rev. Lett. **44**, 1316 (1980).

[7] W.M. Alberico, A. Bottino, and A. Molinari, Phys. Lett. **114B**, 266 (1982); W.M. Alberico, J. Bernabeu, A. Bottino, and A. Molinari, Nucl. Phys. **A429**, 445 (1984); W.M. Alberico, A. De Pace, and M. Pignone, Nucl. Phys. **A523**, 488 (1991).

[8] C.B. Dover, A. Gal, and J.M. Richard, Phys. Rev. D **27**, 1090 (1983); Phys. Rev. C **31**, 1423 (1985); Nucl. Instrum. Methods. Phys. Res., Sect. A **284**, 13 (1989).

[9] J. Huefner and B.Z. Kopeliovich, Mod. Phys. Lett. A **13**, 2385 (1998).

[10] E. Friedman, A. Gal, and J. Mareš, Nucl. Phys. **A761**, 283 (2005).

[11] A. Gal, Phys. Rev. C **61**, 028201 (2000).

[12] K.G. Chetyrkin, M.V. Kazarnovsky, V.A. Kuzmin, and M.E. Shaposhnikov, Phys. Lett. **99B**, 358 (1981).

[13] M. Baldo-Ceolin *et al.*, Phys. Lett. B **236**, 95 (1990); Z. Phys. C **63**, 409 (1994).

[14] K.S. Ganezer, presented at the International Workshop on Search for Baryon and Lepton Number Violations, Berkeley, September 2007 (<http://inpa.lbl.gov/blnv/blnv.htm>).

[15] H. Yoshiki and R. Golub, Nucl. Phys. **A536**, 648 (1992).

[16] B.O. Kerbikov, A.E. Kudryavtsev, and V.A. Lensky, JETP **98**, 417 (2004).

[17] P. Navrátil, Phys. Rev. C **70**, 014317 (2004).

[18] D.J. Millener, J.W. Olness, E.K. Warburton, and S.S. Hanna, Phys. Rev. C **28**, 497 (1983).

[19] G. Fricke *et al.*, At. Data Nucl. Data Tables **60**, 177 (1995).

[20] C.J. Batty, E. Friedman, and A. Gal, Nucl. Phys. **A689**, 721 (2001).

[21] C.J. Batty, Nucl. Phys. **A411**, 399 (1983).

[22] C.Y. Wong, A.K. Kerman, G.R. Satchler, and A.D. MacKellar, Phys. Rev. C **29**, 574 (1984).

[23] E. Friedman and A. Gal, Nucl. Phys. **A658**, 345 (1999).

[24] M. Abramowitz and I.A. Stegun, *Handbook of Mathematical Functions* (Dover, New York, 9th printing 1970), Chap. 10.